Journal of Applied Polymer Science

High electromagnetic interference shielding with high electrical conductivity through selective dispersion of multiwall carbon nanotube in poly (ε-caprolactone)/MWCNT composites

Ranadip Bera, Sandip Maiti, Bhanu Bhusan Khatua
Materials Science Centre, Indian Institute of Technology Kharagpur 721302, India
Correspondence to: B. B. Khatua (E-mail: khatuabb@matsc.iitkgp.ernet.in)

ABSTRACT: This study presents the preparation of electrically conducting poly(ε-caprolactone) (PCL)/multiwall carbon nanotube (MWCNT) composites with very low percolation threshold (p_c). The method involves solution blending of PCL and MWCNT in the presence of commercial PCL beads. The PCL beads were added into high viscous PCL/MWCNT mixture during evaporation of solvent. Here, the used commercial PCL polymer beads act as an 'excluded volume' in the solution blended PCL/MWCNT region. Thus, the effective concentration of the MWCNT dramatically increases in the solution blended region and a strong interconnected continuous conductive network path of CNT−CNT is assumed throughout the matrix phase with the addition of PCL bead which plays a crucial role to improve the electromagnetic interference shielding effectiveness (EMI SE) and electrical conductivity at very low MWCNT loading. Thus, high EMI SE value (∼23.8 dB) was achieved at low MWCNT loading (1.8 wt %) in the presence of 70 wt % PCL bead and the high electrical conductivity of $\sim 2.49\times10^{-2}$ S cm^{-1} was achieved at very low MWCNT loading (∼0.15 wt %) with 70 wt % PCL bead content in the composites. The electrical conductivity gradually increased with increasing the PCL bead concentration, as well as, MWCNT loading in the composites. © 2015 Wiley Periodicals, Inc. J. Appl. Polym. Sci. **2015**, *132*, 42161.

KEYWORDS: composites; molding; morphology

Received 9 December 2014; accepted 1 March 2015
DOI: 10.1002/app.42161

INTRODUCTION

Over the last few years, polymers have been most promising materials in the current science and technology due to its high mechanical and thermal properties, high processibility, light weight and low cost.[1,2] However, the major disadvantage of the polymers is that, most of the polymers are insulating in nature which restricted the application of the polymers in the various fields, such as sensors,[3] aerospace,[4] electronics,[5] device,[6] automobile, electromagnetic interference (EMI) shielding materials,[7] super capacitor,[8] microwave and Li-ion battery etc. Thus, preparation of conducting polymer has been a great challenge and current science has been turned in new direction. In this regard, among the different conducting nanofillers such as carbon black (CB), carbon nanofibre (CNF), carbon nanotube (CNT), and graphene, CNTs are extensively used for the preparation of conducting polymer due to its high electrical conductivity, high thermal and mechanical properties and also high aspect ratio, large surface area. However, poor dispersion of CNTs throughout the matrix polymer limits the preparation of conducting polymer composites at low nanofillers (CNTs) loading. The electrical conductivity of polymer composites strongly depends on the dispersion of the nanofillers, processing condition and nature of the polymer.

Poly(ε-caprolactone) (PCL) is a bio-compatible, bio-degradable, aliphatic, semi-crystalline polyester with good resistance to water, solvents and oil. The addition of electrically conducting filler, such as multiwall carbon nanotube (MWCNT), opens up a number of further possible applications, such as, conducting substrates for the application an extensive range in various fields (EMI shielding, electronic device etc.). The dispersion level of MWCNT is very high in PCL matrix, due to π–π interaction between the aromatic structure of MWCNT and carbonyl group of PCL.[9] Moreover, PCL possess very low melt viscosity and thus very high level of dispersion of MWCNT in the PCL matrix is expected.

Several groups studied EMI shielding effectiveness (SE) for the different polymer composites. Such as, Huang *et al.*[10] prepared epoxy resin/SWCNT composites and achieved ∼20–30 dB EMI SE at ∼15 wt % loading of SWCNT in the X-band region. Ramoa *et al.*[11] reported EMI SE value of ∼(−20) dB for TPU/CNT composites at 10.0 wt % loading of CNT. They measured

EMI SE value in X band region. Pande *et al.*[12] studied the SE of the polycarbonate (PC)/MWCNT composites and the obtained EMI SE value was ~43 dB at ~20 wt % MWCNT loading. Khatua *et al.*[13] prepared PS/GNP/MWCNT composites through *in-situ* polymerization in the presence of PS/GNP bead. They achieved EMI SE value of ~20.2 dB at ~2 wt % loading of MWCNT and 1.5 wt % loading of GNP. Gupta *et al.*[14] prepared PS/MWCNT foam and achieved EMI SE of ~18.2–19.3 dB at ~7 wt % loading of MWCNT. Thomassin *et al.*[15] achieved EMI SE value of PCL/MWCNT composites around ~25 dB at ~1 wt % MWCNT loading. Khatua *et al.*[16] prepared PC/MWCNT nanocomposite through solution blending and achieved 23.1 dB EMI SE value at 2 wt % MWCNT loading.

Several research groups reported the preparation of conducting nanocomposites based on PCL and MWCNT. For instance, Wurm *et al.*[17] achieved electrical conductivity of $\sim 10^{-2}$ S cm^{-1} at ~2 wt % MWCNT loading in melt-mixed PCL/MWCNT composites. Mitchell *et al.*[18] prepared PCL/SWCNT composite by solution blending and achieved electrical conductivity of $\sim 1.5 \times 10^{-3}$ S cm^{-1} at ~3 wt % CNT loading. Saeed *et al.*[19] studied the electrical conductivity of PCL/MWNT composites prepared through *in-situ* polymerization. The obtained conductivity was $\sim 10^{-2}$ S cm^{-1} at ~2 wt % MWCNT loading. Potschke *et al.*[20] prepared PCL/MWCNT composite using melt mixing method. The reported resistivity of the composites was $\sim 10^{4}$ (ohm.cm) at ~3 wt % MWCNT loading. Bello *et al.*[21] reported the electrical conductivity of the PCL/MWCNT composites, prepared by melt blending method. They achieved percolation threshold at ~0.3 wt % CNT loading. Miltner *et al.*[22] studied the percolation threshold for PCL/CNT composite and they achieved percolation threshold at ~0.5 wt % CNT loading. Sayyar *et al.*[23] prepared PCL/graphene composites by solution blending method. They obtained electrical conductivity of $\sim 10^{-2}$ S cm^{-1} at ~10 wt % graphene loading. Villmow *et al.*[24] achieved electrical conductivity in the order of $\sim 10^{-2}$ S cm^{-1} at ~0.7 vol % MWCNT loading for PCL/MWCNT composites. Khatua *et al.*[25] prepared PC/PCL-MWCNT composites by melt blending method. The electrical conductivity of the composites was greatly influenced in the presence of PCL polymer.

In the present study, we prepared PCL/MWCNT composites with high electrical conductivity at extremely low CNT loading through solution blending of PCL and MWCNT in the presence of commercial PCL bead. Here, MWCNTs were selectively dispersed in the solvent dried continuous PCL phase and PCL beads act as an "excluded volume" in the continuous phase in which MWCNT cannot penetrate. Thus, effective concentration of the CNT increases in solution blended PCL region with addition of PCL beads which could improve the EMI SE value as well as electrical conductivity in the composites.

EXPERIMENTAL

Material Details

PCL (CAPA^{TM} 6250, melt flow index, 9 g/10 min, avg. $M_W = 25{,}000$, average diameter ≈3.2 mm and length ≈4.32 mm) was procured from Perstorp, UK. Industrial grade MWCNT (NC 7000 series; average diameter of 9.5 nm and length 1.5 μm; surface area: 250~300 m^2/g; 90% carbon purity) was purchased from Nanocyl S.A., Belgium. We have used PCL as matrix polymer due to its low melt viscosity. This low melt viscosity of PCL facilitates the better dispersion of MWCNT throughout the solvent dried PCL phase which also plays an important role to get the electrical conductivity comparatively at low MWCNT loading. The MWCNT was used as received, without any further chemical modification.

Preparation of PCL/MWCNT Composites

Initially, calculated amount of PCL beads (4 g) were dissolved in dichloromethane (DCM) solvent (15 mL) in a round bottom flask (RB). MWCNT (0.005 g) was sonicated by ultra-sonication in another RB containing DCM solvent (15 mL) for 45 min. Then, the PCL solution was gradually added to the suspension of MWCNT and continued ultra-sonication for another 40 min. After that, the viscous solution of PCL−MWCNT was stirred by magnetic stirrer at 50°C for the evaporation of DCM solvent. After 4 h, when the PCL−MWCNT mixture became highly viscous, 6 g of commercial PCL beads were added into this high viscous PCL−MWCNT mixture under constant stirring. Partial swelling of the PCL beads occurred at the initial stage. Thus, the PCL/MWCNT composites were prepared by solution blending of PCL and MWCNT in the presence of commercial PCL beads. The obtained composites were first air dried and then, kept in an air oven at 50°C for 24 h for drying. From the final weight (~10 g) of the composites, the amount of MWCNT and PCL bead were calculated to be ~0.05 wt % and ~60 wt % loading, respectively. Thus, the (40/60 w/w) (PCL−MWCNT)/PCL composites were prepared with different CNT loadings (~0.03, ~0.05, ~0.10, and ~0.15 wt %) using the same method. The PCL/MWCNT composites with different loadings of PCL bead (~40 to ~70 wt %) at different MWCNT loadings (~0.03, ~0.05, ~0.10, and ~0.15 wt %) were also prepared with the same method. Finally, PCL/MWCNT composites were compression molded at 70°C in a hot press under constant pressure (2 MPa) for further characterizations. The schematic representation for the preparation of the composites is illustrated in Figure 1.

CHARACTERIZATION

Electrical Conductivity

The direct current (DC) conductivity (σ_{DC}) measurement of the composites was done with a four−probe technique on the molded specimen bars of dimensions 30 × 10 × 3 mm^3. The sample was cryogenically-fractured at two ends and the fractured surface was coated with silver (Ag) paste to ensure good contact of the sample surface with electrodes. The specimens were prepared under similar conditions to avoid the influence of the processing parameters on the electrical properties. Minimum of five tests were performed for each specimen and the data was averaged.

The frequency (f) dependent alternating current (AC) conductivity (σ_{AC}) and dielectric permittivity of the composites (disc type sample with thickness 0.3 cm and area $\sim 1.88 \times 10^{-1}$ cm^2) were obtained using a computer controlled precision impedance analyzer (Agilent 4294A) by applying an alternating electric field (amplitude 1 volt) across the sample cell in the f region of ~40Hz to ~10MHz. A parallel plate configuration is used for all the electrical measurements. Molded disc

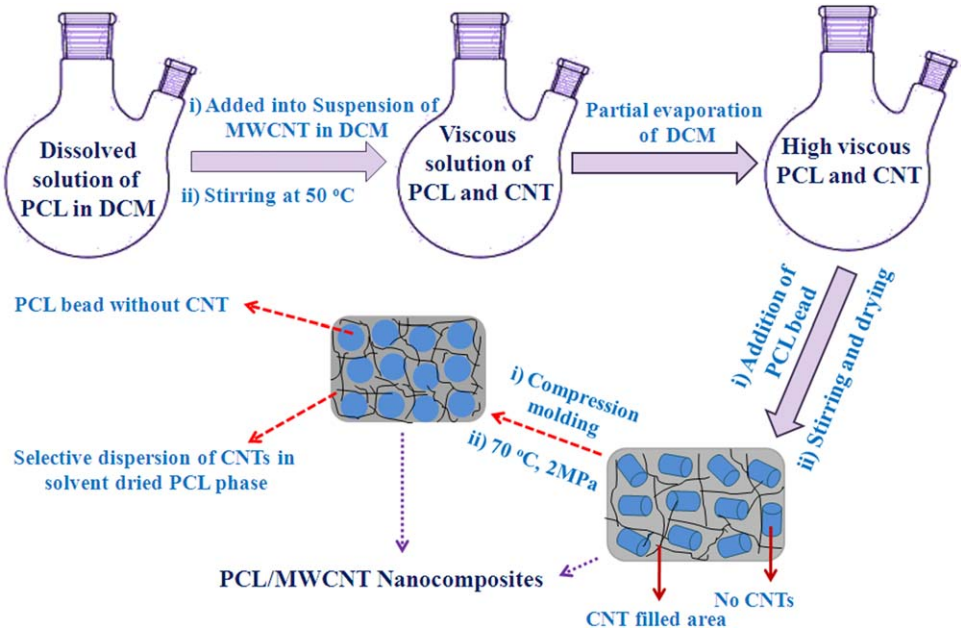

Figure 1. A schematic for the preparation of PCL/MWCNT composites. [Color figure can be viewed in the online issue, which is available at wileyonlinelibrary.com.]

type composites sample was coated with silver (Ag) paste to act as both side electrodes. A sample holder using Platinum (Pt) probe was used for all the electrical measurements.

The parameters like dielectric permittivity (ε') and dielectric loss tangent (tan δ) were obtained as a function of f. The σ_{ac} was calculated from the dielectric data using the relation:

$$\sigma_{ac} = \omega \varepsilon_o \varepsilon' \tan \delta \quad (1)$$

where ω is equal to $2\pi f$, and ε_o is vacuum permittivity. The dielectric permittivity (ε') was determined with the following equation:

$$\varepsilon' = C_p / C_o \quad (2)$$

where C_p is the observed capacitance of the sample (in parallel mode), and C_o is the capacitance of the cell. The value of C_o was calculated using the area (A) and thickness (d) of the sample, following the relation:

$$C_o = (\varepsilon_o \times A)/d \quad (3)$$

EMI SE Measurement

The EMI SE of PCL/MWCNT composites was measured with E5071C ENA series network analyzer (Agilent Technologies) using an industrial standard method. The composites slabs of dimensions 25.5 × 13 × 5.6 mm^3 were measured in the 8.2–12.4 GHz (the so called X band) frequency range.

Optical Microscopy

High resolution optical microscope (HROM, Carl Zeiss Vision GmbH) was used to investigate the distribution of MWCNT and PCL bead in the PCL matrix. Image from the surface of the compression molded sample was taken in monochromatic light at different resolutions.

High Resolution Transmission Electron Microscopy (HRTEM) Analysis

The extent of dispersion of the MWCNT in the PCL matrix was studied by HRTEM (JEM–2100, JEOL, Japan), operating at an accelerating voltage of 200 kV. The PCL/MWCNT composites were ultra-microtomed under cryogenic condition with a thickness of around 60∼90 nm.

Field Emission Scanning Electron Microscopy (FESEM) Study

The surface morphology of the PCL/MWCNT composites was studied using a Carl Zeiss−SUPRATM 40 FESEM, with an accelerating voltage of 5 kV. The molded samples were kept in liquid nitrogen for 30∼50 sec in a stainless steel container and then broken inside the liquid nitrogen. The fractured surfaces of the samples were coated with a thin layer of gold (∼5 nm) to avoid electrical charging. The vacuum was in the order of $\sim 10^{-4}$ to $\sim 10^{-6}$ mm Hg during scanning and FESEM images were taken on the fractured surface of the sample.

RESULTS AND DISCUSSION

EMI SE Measurement

The frequency dependent EMI SE of PCL/MWCNT composites are shown in Figure 2. The EMI SE of the composites were characterized in the X band frequency region (8.2–12.4 GHz). For the evaluation of EMI SE value of any composites or materials, the following equation is generally used:

$$\text{EMI SE(dB)} = 10 \log(P_0/P_t) \quad (4)$$

Where, P_0 is the incident electromagnetic power and P_t signifies the transmitted or remaining electromagnetic power.[26]

The EMI SE value of the PCL/MWCNT composites increases with increasing the MWCNT loading in the X band frequency

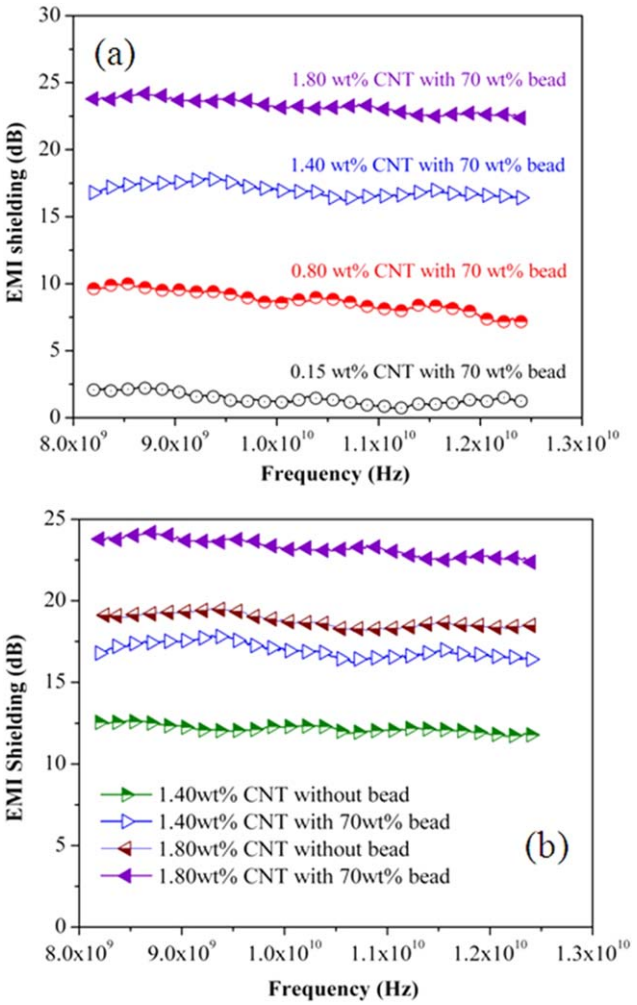

Figure 2. (a) The variation of EMI Shielding with frequency of the PCL/MWCNT composites containing various MWCNT loadings with constant PCL bead loading and (b) the comparative EMI SE values of PCL/MWCNT composites for 1.4 wt % and 1.8 wt % MWCNT loading in the presence of PCL bead loading (70 wt %) and without bead loading. [Color figure can be viewed in the online issue, which is available at wileyonlinelibrary.com.]

region. Thus, the PCL/MWCNT composites show EMI SE value of ~23.8 dB at ~1.8 wt % MWCNT loading with 70 wt % PCL bead content in the X-band region, as shown in Figure 2(a). In general, the minimum EMI SE value of any kind of materials or composites will be around ~20 dB (i.e., equal to or less than 1% transmission of the electromagnetic wave) for commercial applications. Thus, the obtained EMI SE value (~23.8 dB) of the PCL/MWCNT composites fulfilled the criteria of its usefulness in commercial area. This high value of EMI SE of the PCL/MWCNT composites at low MWCNT loading was obtained due to the presence of the commercial PCL bead in the solution blended PCL-MWCNT region. The PCL beads act as an "excluded volume" which increases the effective concentration of the MWCNT in the solvent dried PCL-MWCNT region and greatly improved the EMI SE value of the PCL/MWCNT composites even at low MWCNT loading. Thus, the nano-sized fillers (MWCNT) interact with the incident radiation of the light and act as a crucial role to facilitate easy electron transport throughout the composites. Figure 2(b) shows the comparative EMI SE values of PCL/MWCNT composites for ~1.4 wt % and ~1.8 wt % MWCNT loading in the presence of PCL bead loading (70 wt %) and without bead loading. As observed, the EMI SE values were higher in presence of PCL bead loading (70 wt %) compared to without bead in the composites for both cases. This result indicates that PCL bead plays an 'excluded volume' which increases the effective concentration of MWCNT in the composites. Thus, the EMI SE values of the composites increased with increasing the PCL bead loading. The high electrical conductivity value and continuous conducting interconnected network chains of MWCNT play a crucial role for electrical conduction and improve the EMI-shielding performance of PCL/MWCNT composites as already reported in various literature.[27,28] The enhancement of EMI-shielding value via absorption in the conducting composites occurred due to several factors such as (i) orientation of conducting nanofillers formed a strong interconnected network path among them which increased the electrical conductivity and EMI SE of the composites and, (ii) the more random distribution of conducting nanofillers also plays a key role to increase the EMI SE value of the composites, already been reported.[29] To understand more, a schematic representation has been drawn for the contributions of the absorption and reflection mechanisms to the total EMI SE where the effects of PCL bead was clearly observed on the EMI shielding performance in the PCL/MWCNT composites, as shown in Figure 3. Thus, the obtained EMI SE value of PCL/MWCNT composites with bead loading (70 wt %) is higher compared to the PCL/MWCNT composites without bead at same MWCNT loading (~1.4 and ~1.8 wt % MWCNT), was shown in Figure 2(b). The higher EMI SE value via absorption for the composites with bead loading was explained by two different pathways such as (a) change of conducting nanofillers orientation with minimum breakage of nanofillers which form a strong conducting interconnected network path and increased the electrical conductivity of the composites, resulted high EMI SE value and, (b) multiple reflection which is the electromagnetic wave reflection at various surfaces and interfaces inside the shield,[30] was another shielding mechanism that was affected by the structure. In the PCL/MWCNT composites with bead loading, the entering incident electromagnetic waves were reflected and scattered at the matrix interfaces many times. Thus, this multiple reflection combined with the adequate level of wave absorption capability inside the composite matrix resulting in the further attenuation of electromagnetic waves and thereby improved the EMI SE in the composites.[31] The difference between the wave scattering and multiple reflections in the PCL/MWCNT composites without bead loading [Figure 3(a)] and composites with bead loading [Figure 3(b)] samples is schematically presented in Figure 3.

Generally, the summation of transmissivity (T), reflectivity (R), and absorptivity (A) must be "one," expressed by following relation,

$$T+R+A=1 \quad (5)$$

The transmissivity (T) and reflectivity (R) coefficients were estimated through S parameters and related by the following equation:

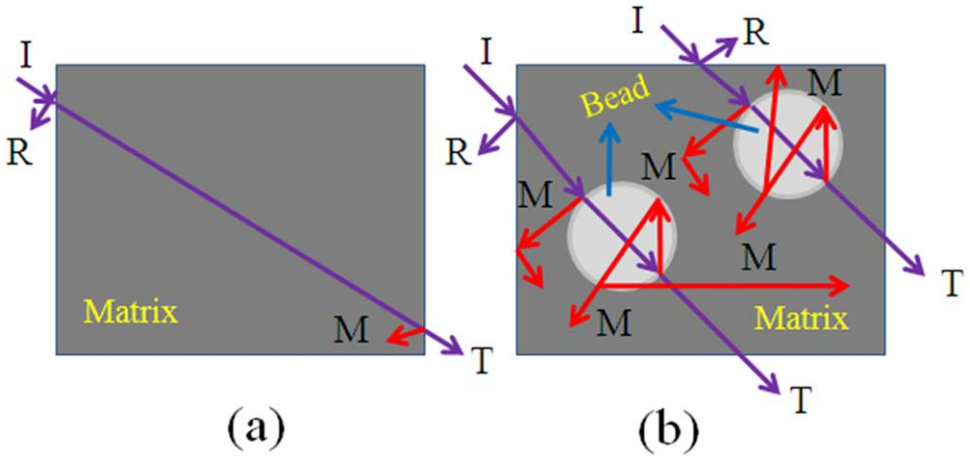

Figure 3. Schematic representation for the difference between the wave scattering and multiple reflections in the PCL/MWCNT composites without bead loading [Figure 3(a)] and composites with bead loading [Figure 3(b)], where I, R, M and T are respectively incident, reflection, multiple internal reflection and transmission of electromagnetic wave. [Color figure can be viewed in the online issue, which is available at wileyonlinelibrary.com.]

$$T=[E_T/E_I]^2=|S_{12}|^2=|S_{21}|^2 \quad (6)$$

$$R=[E_R/E_I]^2=|S_{11}|^2=|S_{22}|^2 \quad (7)$$

With respect to the power of the effective incident electromagnetic wave inside the shielding material, the reflectance and effective absorbance can be conveniently expressed as[32]

$$SE_R=-10\log(1-R) \quad (8)$$

$$SE_A=-10\log(1-A_{eff})=-10\log[T/(1-R)] \quad (9)$$

Using the equations given below,

$$SE_R=-10\log R \quad (10)$$

$$SE_{total}=-10\log T \quad (11)$$

$$A=1-T-R \quad (12)$$

where SE_{total} is total value of EMI SE.

With the help of the above equations, the values of absorptivity (A), reflectivity (R), and transmissivity (T) have been calculated for PCL/MWCNT nanocomposites with ~1.8 wt % MWCNT loading and 70 wt % PCL bead. The obtained values are 0.77 for the reflectivity (R), 0.223 for absorptivity (A), and 0.007 for transmissivity (T), respectively at 8.2 GHz. This result indicated that reflection contributed more than absorption to the EMI SE. Thus, the contribution of reflection to the total EMI SE is much larger than that from absorption which is the primary EMI SE mechanism for nanocomposites in the X-band region. So, this nanocomposite can be used various fields of applications for shielding, such as in construction of light weight shielding room etc.

Electrical Conductivity

σ_{DC} Measurement. The value of σ_{DC} of the PCL/MWCNT composites strongly depends on the amount of the CNT and PCL bead in the composites, as shown in Figure 4. In both cases, the value of σ_{DC} gradually increased with increasing the CNT and PCL bead loading. Figure 4(a) shows the variation of the conductivity value for the different PCL bead amounts (0–70 wt %) at a particular MWCNT loading (~0.15 wt %). As can be seen, the value of σ_{DC} increases gradually with increasing the amount of PCL bead in the composites at constant CNT loading (~0.15 wt % MWCNT loadings). In the absence of any PCL bead, PCL/MWCNT composites showed electrical conductivity of $\sim 3.67 \times 10^{-3}$ S cm^{-1} at ~0.15 wt % MWCNT loading. However, this value ($\sim 3.67 \times 10^{-3}$ S cm^{-1}) increased to $\sim 6.87 \times 10^{-3}$ S cm^{-1} when the composites was prepared with 50 wt % PCL bead. In addition, the composites shows electrical conductivity of $\sim 9.81 \times 10^{-3}$ S cm^{-1} for 60 wt % PCL bead and $\sim 2.49 \times 10^{-2}$ S cm^{-1} for 70 wt % PCL bead at ~0.15 wt % MWCNT loading, respectively. This kind of phenomena of electrical conductivity in the PCL/MWCNT composites was also obtained for all the composites with different loading (~0.03, ~0.05, and ~0.10 wt %) of MWCNT. The change in electrical conductivity of the composites with the variation of PCL bead can be explained by considering the PCL beads as an 'excluded volume' in the composites. In the PCL−MWCNT composite, PCL beads act as an 'excluded volume' where MWCNTs fail to penetrate. Thus, the resultant concentration of MWCNT in the solvent dried continuous PCL phase increased in the presence of PCL beads which helped to achieve incredibly high electrical conductivity even at very low MWCNT loading (~0.03 wt %) in the composites.

Figure 4(b) shows the variation of the σ_{DC} of the composites for various amount of MWCNT loading (~0.03, ~0.05, ~0.10, and ~0.15 wt %) in the absence of any PCL bead content in the solvent dried PCL−MWCNT composite. As can be seen, the value of σ_{DC} of the PCL/MWCNT composites strongly depends on the concentration of the MWCNT loading and increased with increasing the CNT loading. Initially, the PCL/MWCNT composites with ~0.001 wt % MWCNT loading behaves like an insulating materials and shows electrical conductivity of $\sim 1.1 \times 10^{-12}$ S cm^{-1}. However, this low value ($\sim 1.1 \times 10^{-12}$ S cm^{-1}) of σ_{DC} of the composites was greatly improved to $\sim 6.31 \times 10^{-6}$ S cm^{-1} when the composites was prepared with ~0.03 wt % loading of MWCNT. This sudden jump in electrical conductivity from $\sim 10^{-12}$ to $\sim 10^{-6}$ clearly supported the formation of continuous conducting interconnected network paths of CNT−CNT in the composites which

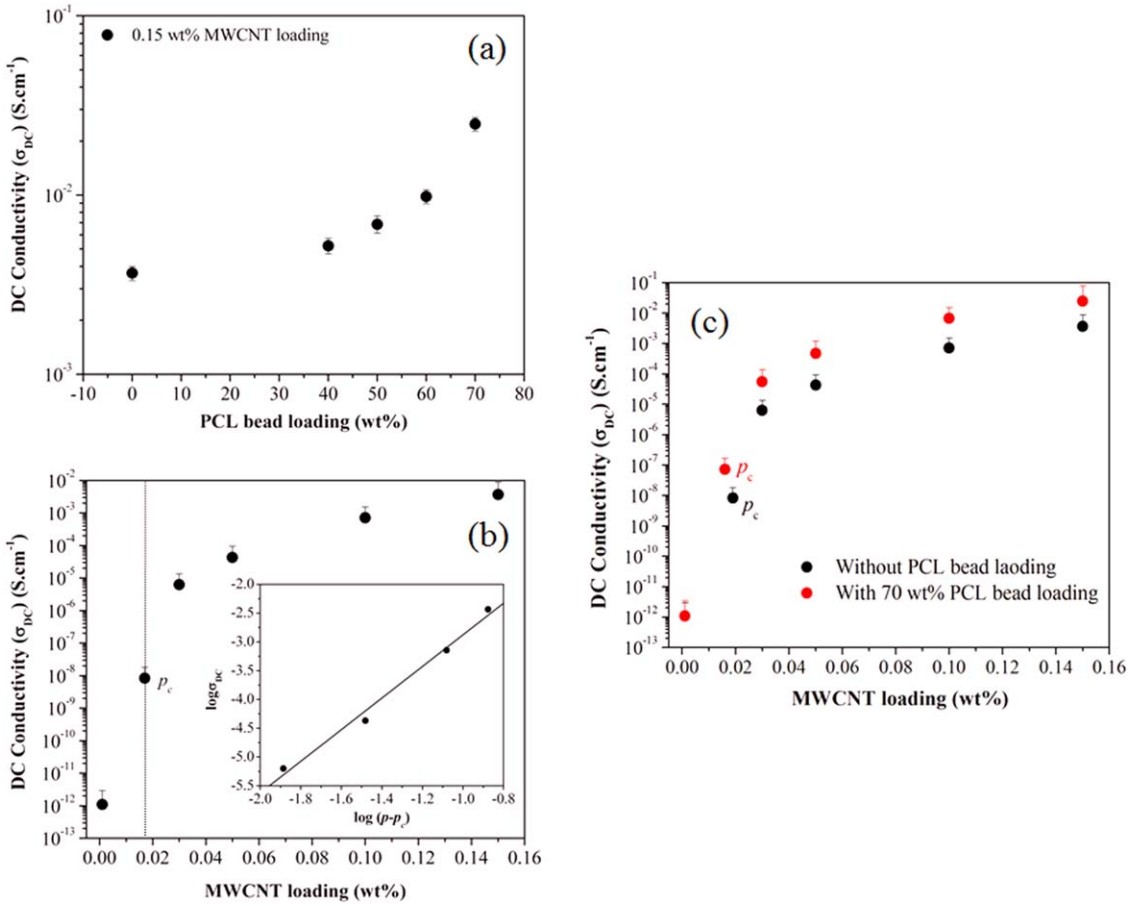

Figure 4. (a) DC conductivity of PCL/MWCNT composites at different weight percent of PCL bead in the PCL matrix with various MWCNT loadings. (b) DC conductivity of PCL/MWCNT composites with MWCNT loading. The log–log plot of σ_{DC} *versus* (p–p_c) for the composites was shown in inset of Figure 4(b). The straight line in the inset is a least–squares fit to the data using eq. (4), giving the best fit values $p_c = \sim 0.019$ wt %. (c) The comparative studies of σ_{DC} of the PCL/MWCNT composites for different MWCNT loading (~0.03, ~0.05, ~0.10 and ~0.15 wt %) in the presence of PCL bead loading (70 wt %) and without bead loading. [Color figure can be viewed in the online issue, which is available at wileyonlinelibrary.com.]

help to conduct the electricity throughout the host polymer. Thus, the obtained value of σ_{DC} of the PCL/MWCNT composites was $\sim 7.16 \times 10^{-4}$ S cm^{-1} at ~0.10 wt % MWCNT loading and $\sim 3.67 \times 10^{-3}$ S.cm^{-1} at ~0.15 wt % of MWCNT loading. With increasing the CNT loading, a strong conducting network structure of CNT–CNT is formed which plays a crucial role to achieve electrical conductivity even at very low CNT loading. Figure 4(c) shows the comparative studies of σ_{DC} of the PCL/MWCNT composites for different MWCNT loading (~0.03, ~0.05, ~0.10 and ~0.15 wt %) in the presence of PCL bead loading (70 wt %) and without bead loading. From the Figure (4c), it is clearly seen that, the values of σ_{DC} were increased in the presence of PCL bead loading. This improvement of electrical conductivity in the presence of bead loading concluded that the effective concentration of MWCNT loading in the solvent dried PCL–MWCNT region increased with increasing the PCL bead loading which acts as an 'excluded volume' in the composites. At constant MWCNT loading, an increase in the weight percent of PCL beads results in a gradual increase in the electrical conductivity of the PCL/MWCNT composites. This increment in weight percent of PCL beads results in the CNT containing part of the composite getting more concise in a smaller area, which increases the continuous conducting interconnected network structure of the CNTs. Thus, addition of PCL bead plays a crucial role to increase the electrical conductivity of the PCL/MWCNT composites at same MWCNT loading and lowers the percolation threshold values (calculated values ~0.016 wt % MWCNT) compared to that (~0.019 wt % MWCNT) of the composites without PCL bead loading.

Several groups[33,34] studied the electrical conductivity of the polymer composites and discussed the electrical conductivity on the basis of percolation theory. The percolation theory suggested that an electrical transition occurred at a particular content of nanofillers loading from insulating materials to conductor which is well known as critical concentration. At this concentration, a continuous conducting interconnected network of nanofillers is developed throughout the insulating polymer matrix which helps to sudden increase in electrical conductivity of the polymer composites, known as percolation threshold (p_c). The value of σ_{DC} of the polymer composites can be expressed by the following scaling law relation:

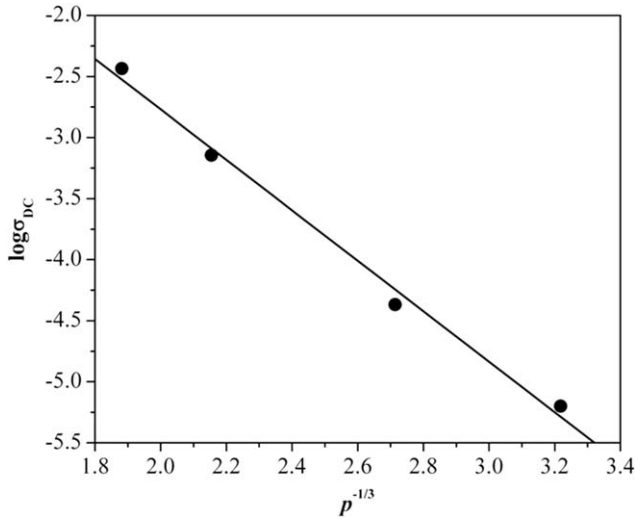

Figure 5. Plot of $\log\sigma_{DC}$ versus $p^{-1/3}$-for PCL/MWCNT composites.

$$\sigma_{DC}(p) \propto (p-p_c)^t \quad \text{For} \quad p > p_c \tag{13}$$

where p is the nanofiller content, "t" is critical exponents.[35] With the help of the eq. (13), $\log\sigma_{DC}$ versus $\log(p–p_c)$ has been drawn and the "t" and "p_c" values are estimated for the PCL/MWCNT composites, as shown in the inset of Figure 4(b). Thus, the obtained values of "t" and p_c were ~2.96 and ~0.019 wt % loading of MWCNT, respectively. This very low p_c value (~0.019 wt % MWCNT) supported the homogeneous dispersion CNT throughout the matrix phase which helped to reduce the p_c value enormously. Moreover, the p_c value of the composites depends on several factors,[36,37] such as, (a) high aspect ratio of MWCNT can reduce the p_c value, (b) high surface area of the CNTs can also reduce the p_c value through tunneling conduction among the conducting nanofillers, (c) the flexible MWCNT can also play a crucial role to decrease the p_c value greatly by developing a physical entanglements between neighboring CNTs through small attractive forces, etc. In this study, we have used superior grade, highly purified MWCNT of high aspect ratio which facilitates the electron conduction throughout the composites. It is noteworthy that, the percolation threshold found in our study is considerably lower (0.019 wt % of MWCNT) than that found previously using SWCNT (0.09 wt % of SWCNT).[16] But, if we look into the DC conductivity at the percolation point, the SWCNT gives significantly high conductivity value (~10^{-7}) than that of using MWCNT in the present study.

According to Balberg *et al.*,[38] the p_c value can be written in terms of average excluded volume (L/R) by the following relation:

$$p_c(L/R) \approx 3 \tag{14}$$

where L is the length of the randomly oriented CNTs and R represents the radius of the CNTs. The percolation theory[39] suggetsed that a continuous conducting network chains of conducting nanofillers has been developed throughout the composites at the critical concentration of the nanofillers. An interparticle conduction is occurred in the conducting polymer composites among the conducting nanofillers which help to develop an electrical conducting path in the composites. Grossiord *et al.*[40] have studied the electrical conductivity of the conducting polymer composites and reported that the tunneling conduction plays an important role behind the electrical conductivity in polymer composites. Ryvkina *et al.*[41] have also studied the electrical conductivity of the polymer/CB composites using the electron tunneling mechanism. They expressed the electrical conductivity on the basis of theoretical model using the following relation:

$$\sigma_{DC} \propto \exp(-Ad) \tag{15}$$

where A is the tunnel parameter and d signifies the width of the potential barrier. The tunneling conduction mechanism[42,43] proposed that the charge carriers can travel among the conducting nanofillers through the conducting polymer composites across insulating polymeric gaps and electrical conductivity of the composites strongly depends on the existence of tunneling conduction in the composites.[44] The current in a tunnel junction depends on the barrier width and it decreases with increasing the barrier width. The nanofillers are supposed to be randomly

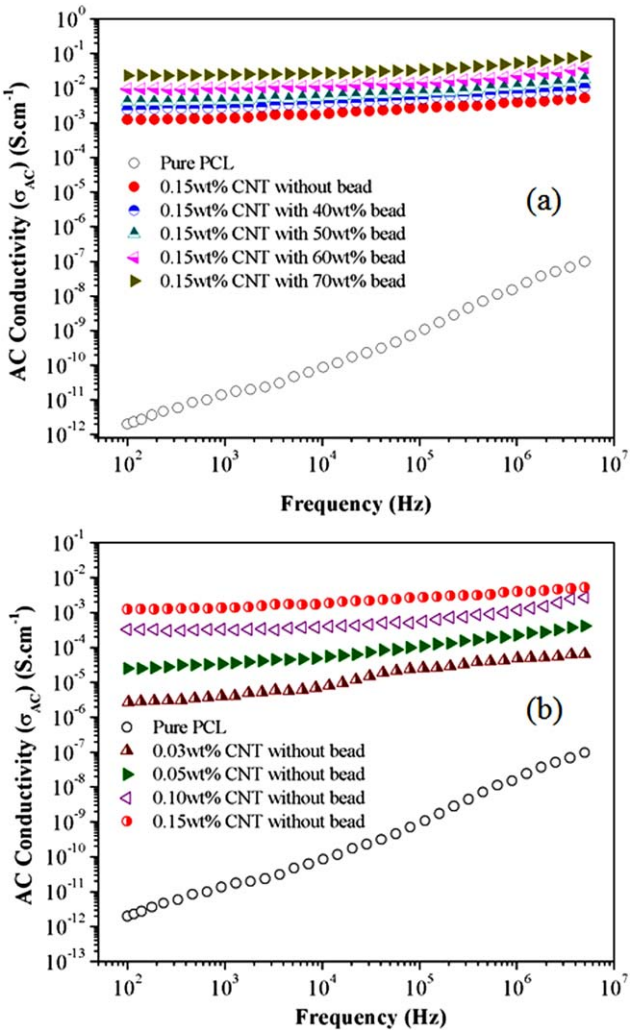

Figure 6. AC conductivity of the PCL/MWCNT composites versus frequency at (a) different loading of PCL bead at constant CNT loading and, (b) different CNT loadings without PCL bead. [Color figure can be viewed in the online issue, which is available at wileyonlinelibrary.com.]

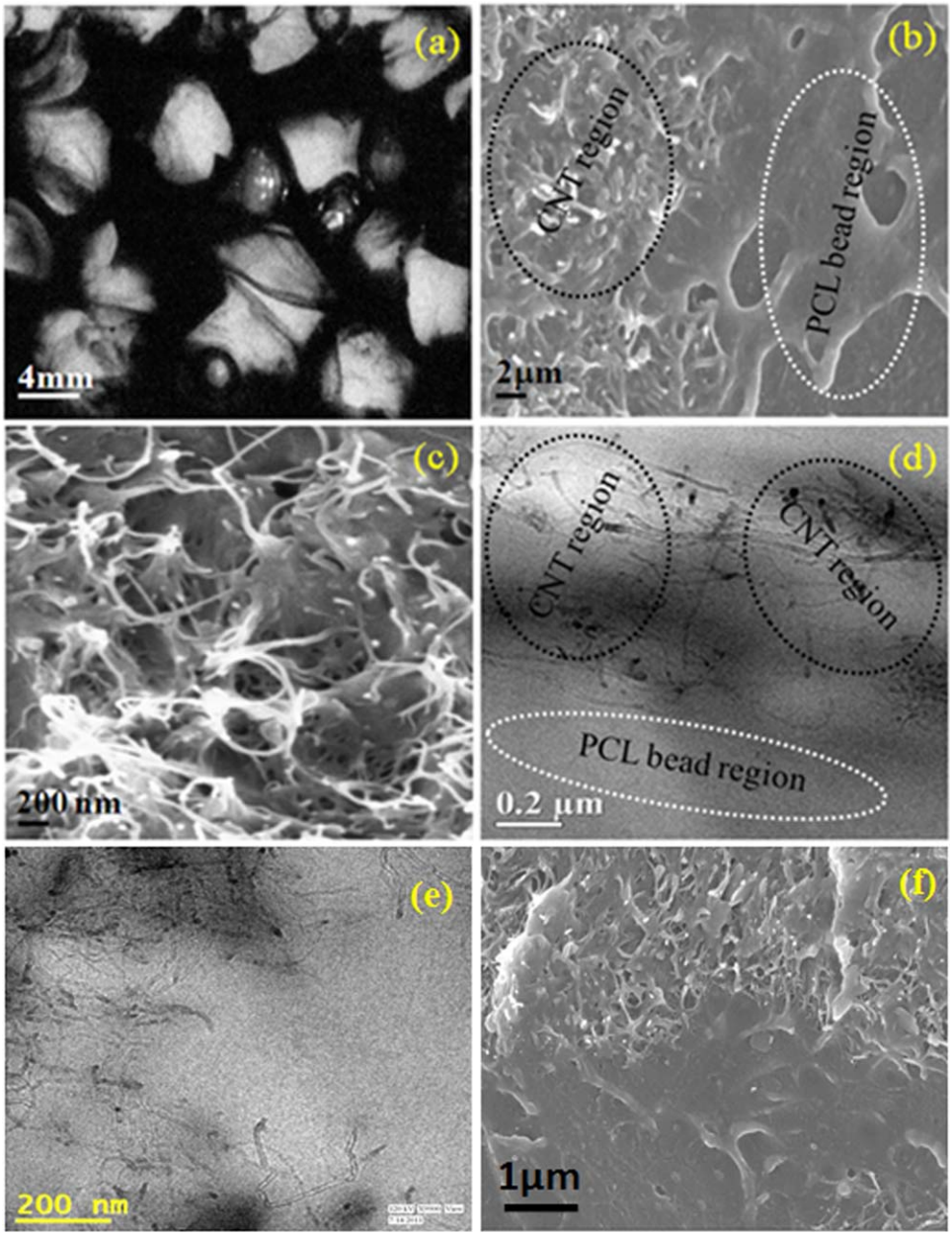

Figure 7. (a) Optical micrograph, (b) & (f) FESEM micrographs of the composites showing CNT region and PCL bead region (c) dispersed MWCNT in the CNT region, and (d) & (e) HRTEM micrograph of PCL/MWCNT composites with 70 wt % PCL bead and 0.15 wt % MWCNT loading. [Color figure can be viewed in the online issue, which is available at wileyonlinelibrary.com.]

oriented throughout the polymer matrix, and the mean average distance (d) among the nanofillers would be considered as barrier width (d). The barrier width is related to the nanofiller concentration in weight, $p^{-1/3}$ by the given relation:[45]

$$d \propto p^{-1/3} \tag{16}$$

Now, using the eqs. (15) and (16) together, the tunneling assisted conductivity ($\log\sigma_{DC}$) of the conducting polymer composites can be written with the help of the following relation:

$$\log(\sigma_{DC}) \propto p^{-1/3} \tag{17}$$

Thus, $\log\sigma_{DC}$ of the eq. (17) has been linearly varied with $p^{-1/3}$, as shown in Figure 5.

This linear variation of $\log\sigma_{DC}$ versus $p^{-1/3}$ indicated the presence of tunneling mechanism behind the electrical conductivity of the PCL/MWCNT composites. Kilbride *et al.*[46] discussed that polymer creates a very thin insulating polymer layer on the individual conducting nanofiller in the conducting polymer composites. So, tunneling of the electrons does not occur between adjacent nanofillers due to the presence of very thin layer of insulating polymer which acts as a high energy barrier. As a result, contact resistance of the nanofillers increased and reduced the electrical conductivity. However, this high energy barrier is reduced when a voltage is applied between the two electrodes which act as a driving force for tunneling conduction among the nanofillers. Thus, the contact resistance among the

adjacent nanofillers reduced and the electrical conductivity of the composites increased.

Measurement of σ_{AC}. The frequency dependent AC electrical conductivity (σ_{AC}) of PCL/MWCNT composites is shown in Figure 6. Figure 6(a) shows the variation of σ_{AC} at different PCL bead content (0–70 wt %) for a particular MWCNT loading (~0.15 wt %) and the value of σ_{AC} increases with increasing the bead loading (up to 70 wt %) at ~0.15 wt % CNT loading. This improvement in σ_{AC} led us to conclude that effective concentration of the CNT increases in the solvent dried PCL–MWCNT phase with increasing the PCL bead content in the composites. It is assumed that strong interconnected conducting network chains of CNT−CNT is formed in the solvent dried PCL/MWCNT region in PCL/MWCNT composites as a result of increasing effective concentration of MWCNT in presence of PCL beads. Addition of PCL bead increase the effective CNT loading acts as an excluded volume. Thus the increases of conductivity occur for the composite with bead compared to without any PCL bead. However, the increase in conductivity in presence of bead also depends on the loading of the bead. At higher loading the composite contain more insulating PCL bead and then CNT dispersed in a smaller region and thus expected to have less branching of continuous CNT network. At relative lower loading, more CNT containing region will be available in the composite which leads to more network of CNT in the composite matrix. Thus significant increase in conductivity is not observed with bead containing.

Figure 6(b) shows the variation of σ_{AC} of the PCL/MWCNT composites at different MWCNT loadings (~0.03 to ~0.15 wt %) in the absence of PCL bead content. As observed, the value of σ_{AC} also improved with increasing the amount of CNT loading. This is the general phenomena of the conducting materials.[47] With increasing the MWCNT loading, a continuous conductive interconnected network path is developed which helps to conduct the electricity throughout the composites. Thus, AC electrical conductivity of the composites gradually increases with increasing the CNT loading in the composites.

Morphology

Figure 7 shows the different morphological images of the PCL/MWCNT composites. The optical micrograph image of the composites with 0.15 wt % of MWCNT in the presence of 70 wt % PCL beads was studied and observed the two phase regions in Figure 7(a). As observed, a continuous opaque phase (black phase in the image) which is indication of the solution blended PCL–MWCNT region and the existence of the pure PCL bead region without any kind of CNT was supported by the transparent regions of the optical micrograph in Figure 7(a). Thus, two phase regions (pure PCL bead phase and PCL–MWCNT solvent dried phase) in the PCL/MWCNT composites were confirmed by this optical micrograph. Here, the size of the PCL bead is reduced to some extent in the composites which could be due to partial swelling and surface etching of the PCL beads by the solvent during preparation of the PCL/MWCNT composites. The FESEM images of the PCL/MWCNT composites with ~0.15 wt % MWCNT in the presence of 70 wt % PCL bead were also characterized to observe the two phase regions in the composites, as shown in Figure 7(b,c,f). The Figure 7(b,f) clearly shows the two phase regions, where MWCNTs are dispersed in the solvent dried PCL phase and CNT free rest of the phase suggested the existence of PCL bead regions in the composites. Thus, this image unambiguously led us to conclude that MWCNTs were selectively dispersed in the solvent dried PCL phase, and failed to penetrate inside the PCL bead regions during the preparation of composites in the presence of PCL beads. In addition, PCL bead acts as an "excluded volume" which increases the effective CNT concentration in the solvent dried PCL regions that helps to increase the electrical conductivity of the composites even at a low CNT content. Figure 7(c) is the high magnification FESEM image of the solvent dried PCL–MWCNT phase. This image [Figure 7(c)] indicated the homogeneous dispersion of the CNTs in the solvent dried PCL phase. The HRTEM micrograph of the PCL/MWCNT composites was also studied to check the microstructure in the composites, as shown in Figure 7(d,e). From this image [Figure 7(d,e)], the presence of two phase regions and selective localizations of CNTs in the solvent dried PCL–MWCNT phase can be seen. Thus, all these micrograph images confirmed the selective localizations of CNTs in the composites which developed continuous interconnected network chains of CNT–CNT throughout the matrix phase and plays a key role to improve the electrical conductivity of the composites.

CONCLUSION

In conclusion, a modified conventional solution blending method was demonstrated for the preparation of high electrically conductive PCL/MWCNT composites with very low percolation threshold. The method involves selective localization of MWCNT through solution blending of PCL−MWCNT in the presence of commercial PCL beads. The existence PCL beads in the composites act as an 'excluded volume' where CNTs cannot penetrate during the preparation of the composites. Thus, the effective concentration of the CNTs in the solvent dried PCL−MWCNT phase greatly increases with the incorporation of insulating PCL bead in the composites which leads to achieve high EMI SE and electrical conductivity even at low CNT content. Thus, high EMI SE value (~23.8 dB) was achieved for PCL/MWCNT composites at low MWCNT loading (1.8 wt %) with 70 wt % PCL bead. Additionally, very high electrical conductivity (~2.49×10^{-2} S cm^{-1}) was achieved at very low (~0.15 wt %) CNT loading in the presence of 70 wt % PCL bead with very low percolation threshold (~0.019 wt %), which is not reported till date in PCL/MWCNT composites. Morphological study of the composites confirmed the selective localization of the CNTs in the solvent dried continuous PCL phase and forms infinite numbers of conducting network chains of CNT−CNT in the composites.

ACKNOWLEDGMENTS

The authors thank the University Grant Commission (UGC), New Delhi, India for their financial support.

REFERENCES

1. Li, C. Y.; Li, L.; Cai, W.; Kodjie, S. L.; Tenneti, K. K. *Adv. Mater.* **2005**, *17*, 1198.
2. Fladin, F.; Prasse, T.; Schueler, R.; Schulte, K.; Bauhofera, W.; Cavaille, J. Y. *Phys. Rev. B* **1999**, *59*, 14349.
3. Rahman, R.; Servati, P. *IEEE Transactions on Nanotech.* **2015**, *14*, 118.
4. Araujo, R.; Marques, M. F. V.; Jonas, R.; Grafova, I.; Grafov, A. *J. Nanosci. Nanotechnol.* **2015**, *15*, 6176.
5. Männl, U.; Berg, C. V. D.; Magunje, B.; Härting, M.; Britton, D. T.; Jones, S.; Staden, M. J. V.; Scriba, M. R. *Nanotechnology* **2014**, *25*, 094004.
6. Kaur, R.; Tripathi, S. K. *Microelectronic Eng.* **2015**, *133*, 59.
7. Yousefi, N.; Sun, X.; Lin, X.; Shen, X.; Jia, J.; Zhang, B.; Tang, B.; Chan, M.; Kim, J. K. *Adv. Mat.* **2014**, *26*, 5480.
8. Sidhu, N. K.; Rastogi, A. C. *Nanoscale Res. Lett.* **2014**, *9*, 453.
9. Thomassin, J. M.; Lou, X.; Pagnoulle, C.; Saib, A.; Bednarz, L.; Huynen, I.; Jerome, R. Detrembleur, *C. J. Phys. Chem. C* **2007**, *111*, 11186.
10. Huang, Y.; Li, N.; Ma, Y.; Du, F.; Li, F.; He, X.; Lin, X.; Gao, H.; Chen, Y. *Carbon* **2007**, *45*, 1614.
11. Ramoa, S. I. D.; Barra, G. M. O.; Oliveira, R. V. B.; Oliveira, M. G. D.; Cossad, M.; Soaresd, B. G. *Polym. Int.* **2013**, *62*, 1477.
12. Pande, S.; Chaudhary, A.; Patel, D.; Singh, B. P.; Mathur, R. B. *RSC Adv.* **2014**, *4*, 13839.
13. Maiti, S.; Shrivastava, N. K.; Suin, S.; Khatua, B. B. *ACS Appl. Mater. Inter.* **2013**, *5*, 4712.
14. Yang, Y.; Gupta, M. C. *Nano Lett.* **2005**, *5*, 2131.
15. Thomassin, J. M.; Pagnoulle, C.; Bednarz, L.; Huynen, I.; Jérômea, R.; Detrembleura, C. *J. Mater. Chem.* **2008**, *18*, 792.
16. Maiti, S.; Suin, S.; Shrivastava, N. K.; Khatua, B. B. *RSC Adv.* **2014**, *4*, 7979.
17. Wurm, A.; Lellinger, D.; Minakov, A. A.; Skipa, T.; Potschke, P.; Nicula, R.; Alig, I.; Schick, C. *Polymer* **2014**, *55*, 2220.
18. Mitchell, C. A.; Krishnamoorti, R. *Macromolecules* **2007**, *40*, 1538.
19. Saeed, K.; Park, S. Y. *J. Appl. Polym. Sci.* **2007**, *104*, 1957.
20. Potschke, P.; Kobashi, K.; Villmow, T.; Andres, T.; Paiva, M. C.; Covas, J. A. *Compos. Sci. Technol.* **2011**, *71*, 1451.
21. Bello, A.; Laredo, E.; Marval, J. R.; Grimau, M.; Arnal, M. L.; Muller, A. *J. Macromolecules* **2011**, *44*, 2819.
22. Miltner, H. E.; Watzeels, N.; Block, C.; Gotzen, N. A.; Assche, G. V.; Borghs, K.; Durme, K. V.; Mele, B. V.; Bogdanov, B.; Rahier, H. *Eur. Polym. J.* **2010**, *46*, 984.
23. Sayyar, S.; Murray, E.; Thompson, B. C.; Gambhir, S.; Officer, D. L.; Wallace, G. G. *Carbon* **2013**, *52*, 296.
24. Villmow, T.; Kretzschmar, B.; Potschke, P. *Compos. Sci. Technol.* **2010**, *70*, 2045.
25. Maiti, S.; Suin, S.; Shrivastava, N. K.; Khatua, B. B. *Polym. Eng. Sci.* **2014**, *54*, 646.
26. Wang, J.; Xiang, C.; Liu, Q.; Pan, Y.; Guo, J. *Adv. Funct. Mater.* **2008**, *18*, 2995.
27. Zhang, H. B.; Zheng, W. G.; Yan, Q.; Jiang, Z. G.; Yu, Z. Z. *Carbon* **2012**, *50*, 5117.
28. Ameli, A.; Jung, P. U.; Park, C. B. *Carbon* **2013**, *60*, 379.
29. Zhang, H. B.; Yan, Q.; Zheng, W. G.; He, Z. *ACS Appl. Mater. Inter.* **2011**, *3*, 918.
30. Al-Saleh, M. H.; Sundararaj, U. T. *Carbon* **2009**, *47*, 1738.
31. Ameli, A.; Nofar, M.; Wang, S.; Park, C. B. *ACS. Appl. Mater. Inter.* **2014**, *6*, 11091.
32. Connor, M. T.; Roy, S.; Ezquerra, T. A.; Calleja, F. J. B. *Phys. Rev. B* **1998**, *57*, 2286.
33. Du, F.; Scogna, R. C.; Zhou, W.; Brand, S.; Fischer, J. E.; Winey, K. I. *Macromolecules* **2004**, *37*, 9048.
34. Maiti, S.; Khatua, B. B. *J. Nanosci. Nanotechnol.* **2011**, *11*, 8613.
35. Wu, T. M.; Chen, E. C. *Compos. Sci. Technol.* **2008**, *68*, 2254.
36. Shrivastava, N. K.; Kar, P.; Maiti, S.; Khatua, B. B. *Polym. Int.* **2012**, *61*, 1683.
37. Maiti, S.; Khatua, B. B. *RSC. Adv.* **2013**, *3*, 12874.
38. Balberg, I.; Binenbaum, N.; Wagner, N. *Phys. Rev. Lett.* **1984**, *52*, 1465.
39. Weber, M.; Kamal, M. R. *Polym. Compos.* **1997**, *18*, 711.
40. Grossiord, N.; Loos, J.; Van, L. L.; Maugey, M.; Zakri, C.; Koning, C. E.; Hart, A. *J. Adv. Funct. Mater.* **2008**, *18*, 3226.
41. Ryvkina, N.; Tchmutin, I.; Vilcakova, J.; Peliskova, M.; Saha, P. *Synth. Met.* **2005**, *148*, 141.
42. Wu, D.; Zhang, Y.; Zhang, M.; Yu, W. *Biomacromolecules* **2009**, *10*, 417.
43. Wang, M.; Li, B.; Wang, J.; Bai, P. *Polym. Adv. Technol.* **2011**, *22*, 1738.
44. Laredo, E.; Grimau, M.; Bello, A.; Wu, D. F.; Zhang, Y. S.; Lin, D. P. *Biomacromolecules* **2011**, *11*, 1339.
45. Moniruzzaman, M.; Winey, K. I. *Macromolecules* **2006**, *39*, 5194.
46. Kilbride, B. E.; Coleman, J. N.; Fraysse, J.; Fournet, P.; Cadek, M.; Drury, A.; Hutzler, S.; Roth, S.; Blau, W. J. *J. Appl. Phys.* **2002**, *92*, 4024.
47. Dyre, J. C.; Schroder, T. B. *Rev. Mod. Phys.* **2000**, *72*, 873.